Development 121,173-187 (1995)
Printed in Great Britain © The Company of Biologists Limited 1995

Mechanisms of cell rearrangement and cell recruitment in *Drosophila* ovary morphogenesis and the requirement of *bric à brac*

Dorothea Godt and Frank A. Laski

Molecular Biology Institute, Department of Biology, University of California, Los Angeles, Los Angeles, California 90024, USA

SUMMARY

The *Drosophila* ovary consists of repeated units, the ovarioles, where oogenesis takes place. The repetitive structure of the ovary develops de novo from a mesenchymal cell mass, a process that is initiated by the formation of a two-dimensional array of cell stacks, called terminal filaments, during the third larval instar. We have studied the morphogenetic process leading to the formation of terminal filaments and find that this involves recruitment, intercalation and sorting of terminal filament cells. Two other types of cell stacks that participate in ovary morphogenesis, the basal stalks and interfollicular stalks, also form by cell rearrangement utilizing a convergence and extension mechanism. Terminal filament formation depends on the Bric à brac protein, which is expressed in the nuclei of terminal filament cells and is cell autonomously required. Disruption of terminal filament formation, together with defects of basal and interfollicular stalk development, leads to disruption of ovariole formation and female sterility in *bric à brac* mutants.

Key words: *Drosophila*, *bric à brac*, ovary, terminal filament, convergence and extension

INTRODUCTION

The distinctive and reproducible structure, shape and size of an organ or a whole animal is controlled by the morphogenetic properties of the participating cells. Large scale changes in the shape of a tissue originate from local changes in cell behavior. Changes in cell shape, cell rearrangement and migration have been shown to drive morphogenetic movements during development. Examples in *Drosophila* include gastrulation (Leptin and Grunewald, 1990; Costa et al., 1994), germband extension (Irvine and Wieschaus, 1994), endoderm migration (Reuter et al., 1993; Tepass and Hartenstein, 1994) and imaginal disc evagination (Condic et al., 1991). Most of the work on morphogenetic mechanisms in *Drosophila* has been focused on epithelial sheets. However, studies predominantly done on vertebrates show that mesenchymal cells also participate actively and autonomously in morphogenetic movements and pattern formation during organogenesis (for review see Bard, 1990). One organ where the morphogenetic abilities of mesenchymal cells can be studied genetically is the *Drosophila* ovary.

The *Drosophila* ovary possesses about twenty ovarioles, repeated units that serve as an assembly line for oogenesis (for review see Snodgrass, 1935; King, 1970; Mahowald and Kambysellis, 1980; Spradling, 1993). Each ovariole contains a germarium at its anterior end where oogonia are located, and the 16-germ-cell cyst is formed and surrounded by a follicular epithelium (Fig. 1). The germarium is followed posteriorly by a string of follicles of advancing developmental stages, each of which contains a differentiating oocyte accompanied by fifteen nurse cells. The ovarioles are separated from each other by epithelial sheaths. The different elements of the ovariole are linked together by three specialized cell groups of mesodermal origin, the terminal filament, the basal stalk and the interfollicular stalk. Morphologically similar, each of these is a stack of aligned disc-shaped cells. The terminal filament connects the germarium with the surrounding ovariole sheath, the interfollicular stalks interconnect the follicles, and the basal stalk, which is a transient structure during the pupal stages, attaches the most advanced follicle to a basal cell population at the posterior end of the ovary (King, 1970; Fig. 1).

When the *Drosophila* gonads form during embryogenesis, they have a simple structure containing approximately ten primordial germ cells which are intermingled with and surrounded by mesodermal cells (for review see Campos-Ortega and Hartenstein, 1985). During most of the larval stages, the *Drosophila* ovary consists of a growing spherical mass of mesenchymal somatic and primordial germ cells (Kerkis, 1930), and is transformed through complex morphogenetic events into an organ of repeated units, the ovarioles, during the late larval and early pupal stages (Kerkis, 1933; King et al., 1968; King, 1970). The morphogenetic process that leads to the development of the ovarioles starts with the formation of a field of cell stacks, the two-dimensional array of terminal filaments. Subsequently, anteriorly located somatic cells migrate posteriorly, initially guided by the regular grid provided by the terminal filaments, and subdivide the ovary into ovarioles.

We have studied the development of the terminal filaments and their regular spatial arrangement, as well as the formation of the structurally related basal and interfollicular stalks. We find that they develop through recruitment and cell intercalation of mesenchymal cells, a process resembling the formation of the notochord by convergence and extension in a chordate

embryo (for review see Keller et al., 1992). Furthermore, we show that the pattern forming process through which multiple terminal filaments arise from a common cell population requires cell sorting and we propose a model describing how this might occur. In addition, we find that the *Drosophila* gene *bric à brac* (*bab*) is cell autonomously required for the formation of terminal filaments and is crucial for normal morphogenesis of the ovary. *bric à brac* has previously been shown to be required for proper segmentation and specification in leg primordia, and encodes a nuclear protein which contains a BTB domain, a conserved domain that is found in several transcriptional regulators (Godt et al., 1993; Zollman et al., 1994).

MATERIALS AND METHODS

Drosophila stocks

The P-element-induced *bab* alleles bab^{P}, bab^{PRDS}, bab^{PR24} and bab^{PR72}, and the deficiency *Df(3L)*bab^{PG} were linked with *e ry ca* and maintained as *TM6B, Tb e ca* balanced stocks (Godt et al., 1993). The bab^{A128} *ry* chromosome (Bellen et al., 1989; Godt et al., 1993) is homozygous viable and fertile. The enhancer trap lines P[ry^{+},*lacZ*] AD47 and P[ry^{+},*lacZ*] XA42 (Laski, unpublished), and P[w^{+},*lacZ*] B1-93F (Ruohola et al., 1991) were used as genetic markers for terminal filament cells, and P[w^{+},*lacZ*] B1-93F also for interfollicular stalk cells. Flies used for the mosaic analysis are described below. Balancer chromosomes carried the dominant larval markers *Tb* or *Bc* and are described with other genetic markers in Lindsley and Zimm (1992). Oregon R was used as a wild-type stock. Flies were raised at 25°C on standard *Drosophila* medium.

Mosaic analysis of larval ovaries

Site-directed mitotic recombination was catalyzed by the heat-shock inducible FLP yeast recombinase at a FRT target element (Golic, 1991). The FRT2A insertion, which contains a w^{+} gene and maps proximal to *bab* was recombined with both bab^{A128} and bab^{PRDS} which express β-galactosidase (β-gal) in terminal filament cells. For the experiment *w;* bab^{A128} *FRT2A* and *w;* bab^{PRDS} *FRT2A/ TM6B, Tb* females were crossed to *w; FLP/+; FRT2A/+* males. As a control, females of the same genotype were crossed to *w; +; FRT2A* males. Eggs were collected for 3-5 hours in yeasted vials and the developing animals were kept at 25°C before and after the 2 hours heat shock at 38°C (air incubator). The heat shock was set 48, 60, 72 or 96 hours after oviposition, which corresponds to the early second, mid second, early third and mid third larval instar, respectively. 25% of all female larvae (bab^{A128} experiment) or of those that do not have the dominant *Tb* marker (bab^{PRDS} experiment) are of the genotype *w; FLP/+; bab FRT2A/+ FRT2A* which enables mitotic recombination between non-sister chromatids. In the case of a heat shock at the early second larval instar, the probability (*P*) that a mosaic patch in an ovary is due to a single mitotic recombination event was calculated according to the equation: $P+P2+P3...=P/(1-P)=0.18$, the percentage of mosaic ovaries (see Table 1). For this equation $P=0.1525$, therefore 85% of the mosaic ovaries (0.1525/0.18) are due to a single recombination event. Ovaries were dissected from early prepupae (when terminal filament differentiation is complete) and stained with an anti-β-gal antibody.

Ovary preparation

Adult ovaries were dissected from 2-4 days old well-fed females. To isolate ovaries of specific developmental stages, eggs were collected on apple juice agar plates for 2 hours, and the hatched larvae were fed fresh yeast while growing at 25°C, selected at the second molt or at puparium formation and kept on fresh plates until dissection. Female larvae were recognized by the size of their gonads (Ashburner, 1989). Ovaries were dissected in phosphate-buffered saline (PBS) by opening the larva in the middle of the abdomen and pulling out the fat body to which the ovaries are connected. The fat body, or as in the case of pupae the whole inner content of the posterior body half, was directly transferred into plastic mesh baskets in microtiter plates with PBS on ice, where fixation and antibody incubations were performed. The final staining reaction was done in a glass dish. The ovaries were separated from the fat body with a fine needle in the medium in which they were mounted.

Stainings of ovaries

Antibody stainings were done as described in Godt et al. (1993). Primary antibodies were: anti-Armadillo (1: 200; monoclonal line N2-7A1; Peifer et al., 1994); anti-Bab r2 (1: 1600; Godt et al., 1993); anti-β-gal (1: 3000; polyclonal; Cappel); anti-Fasciclin III (1: 5; monoclonal line 2D5; Patel et al., 1987). Secondary antibodies were either FITC-conjugated or Biotin-conjugated (Jackson Laboratories) and were preabsorbed to a mixture of biobeads (Bio-Rad, Kuo et al., 1982) and embryos for 1 hour before usage.

To monitor β-gal activity, ovaries were fixed in 0.5% glutaraldehyde in PBS for 10 minutes, washed in PBS and incubated in prewarmed X-gal staining solution (Bellen et al., 1989) containing 0.1% X-gal (Bachem) at 37°C for 2-3 hours. For detection of actin filaments, formaldehyde fixed ovaries were incubated in 10 units/ ml rhodamine-phalloidin (Molecular Probes) in PBS overnight at 4°C. Cell nuclei were visualized by treatment with 1 μg/ ml diamino-2-phenylindole (DAPI, Sigma) in PBS for 30 minutes after X-gal staining or directly after fixation.

Ovaries were mounted in 50% glycerol-PBS for classic microscopy, in 80% glycerol-PBS for confocal microscopy and in an Epon/Araldite mixture for histological sectioning (4 μm). Pictures were taken with a Zeiss Axioskop microscope equipped with Nomarski and fluorescence optics. Confocal images were obtained using a Bio-Rad MRC-600 Confocal laser scanner, mounted on a Nikon Diaphot microscope, and CoMOS software (Biorad).

RESULTS

Development of cell stacks during ovary morphogenesis

During the third larval instar distinct mesodermal cell populations become apparent in the ovary. By puparium formation the different cell populations are arranged in layers along the anterior-posterior axis (King, 1970; Fig. 1A). There are three cell populations in the anterior region of the ovary. The anterior most cells, which we refer to as cap cells, participate in the formation of the peritoneal sheath which envelops the whole ovary. The apical cells migrate between the terminal filaments and form the epithelial sheaths that divide the ovary into ovarioles. Terminal filaments are already differentiated cell stacks. The central region is occupied by the germ cells intermingled with somatic cells that are believed to give rise to the precursors of the follicle cells and the interfollicular stalk cells in the germarium. The posterior region consists of at least two distinct cell populations: the basal stalk primordium and the basal cells that will form the calyx of the oviduct. During the larval and prepupal stages the fat body is attached to the lateral side of an ovary.

Three types of cell stacks are found in a pupal ovary (Fig. 1B), and each forms at a different stage of ovary development. The terminal filaments (TFs), stacks of 8-9 cells, form during the third larval instar. King (1970) mentions that short TFs have already formed at mid third larval instar. The basal stalks

(BSs), stacks of approximately 30 cells, are made during the early pupal phase; and the interfollicular stalks (IFSs), each of which comprises 6-8 cells, are generated from the mid pupal stage onward.

Terminal filaments develop successively along the anterior-posterior and medial-lateral axis

At onset of metamorphosis all TFs (around 20) have differentiated, each of them a stack of 8-9 aligned disc-shaped cells that are oriented along the anterior-posterior axis of the ovary. The stacks are arranged in a plane along the dorsal-ventral and medial-lateral axis. The Bab protein is expressed in the nuclei of TF cells and in 2-3 somatic cells that are located at the base of each TF but are not aligned with the TF cells (Fig. 2A). Bab is expressed in TF cells before they differentiate to disc-shaped cells and we have used an anti-Bab antibody to study the process of TF formation.

TFs form in the third larval instar beginning approximately 12 hours after the second molt and finishing 36 hours later shortly before puparium formation. Stacks emerge in a two-dimensional pattern which is oriented along the medial-lateral and dorsal-ventral axis. The first two stacks begin to form on the medial side of the ovary (Fig. 2B). Slightly later a crescent-like staining is seen across the medial half of the ovary (Fig. 2C). A short stack of 5-6 aligned cells with flattened nuclei has formed on the medial side with cell clusters of decreasing size and irregular shape located more laterally. During the following 24 hours, new TFs appear more and more laterally and the older stacks increase in size (Fig. 3E). Approximately 32 hours after the second molt, the last TFs begin to develop at the lateral side of the ovary. These observations show that TFs form progressively from the medial to the lateral side of the ovary and that individual TFs develop gradually through an increase of their cell number (illustrated in Fig. 3H). This is consistent with observations from enhancer trap lines which label TF cells (Sahut, Godt, Laski and Couderc, unpublished data).

TF formation can be divided into four stages. These stages are most easily distinguished along the dorsal-ventral axis where rows of TFs develop simultaneously (summarized in Fig. 3H).

(Stage 1) TF cells have a spindle-like shape and are not organized in clusters but appear as a uniform cell layer along the dorsal-ventral axis (Fig. 3A). This cell layer lies between the anteriorly located apical cells and the posteriorly located germ cells. The beginning of TF formation is marked by the appearance of a furrow around the TF region, which indicates that TF cells leave the surface and move to the interior of the ovary (Fig. 3A,B).

(Stage 2) Clusters of each 5-6 strongly stained TF cells appear next to each other (Fig. 3B,F). The formation of clusters from the uniform cell population seems to occur by cell intercalation. These clusters have an eye-shaped appearance and differ from a mature TF by a smaller cell number, spindle-shaped cells and non-aligned cell nuclei.

(Stage 3) The clusters increase in size to the final number of 8-9 TF cells (Fig. 3C,G), which we show below to occur by cell recruitment. The process is initiated by the appearance of weakly stained TF cells posterior to the clusters (Fig. 3F). These cells join individual clusters leading to clusters of increased size.

(Stage 4) TF cells change their shape, their tapered ends becoming blunt and their nuclei almost perfectly aligned, resulting in a mature TF (Fig. 3D).

Changes in cell shape are accompanied by alterations in the distribution of actin filaments and Armadillo during terminal filament formation

To understand better how distinct TF cell clusters are formed, ovaries were stained with phalloidin, which binds to actin filaments. Before cluster formation begins, TF cells and apical cells, which are located in a layer anterior to the TF cells, cannot be distinguished from one another in phalloidin stainings because they both have a similar spindle-like shape (Fig. 4A). In early stage 2, the TF cells of prospective neighboring clusters are interdigitated with each other along the dorsal-ventral axis (Fig. 4B). Actin filaments are homogeneously distributed beneath the surface of the cells. To form distinct clusters, the cells of adjacent stacks sort out from one another. This sorting process is immediately followed by a strong bundling of the tapered ends of these cells, which leads

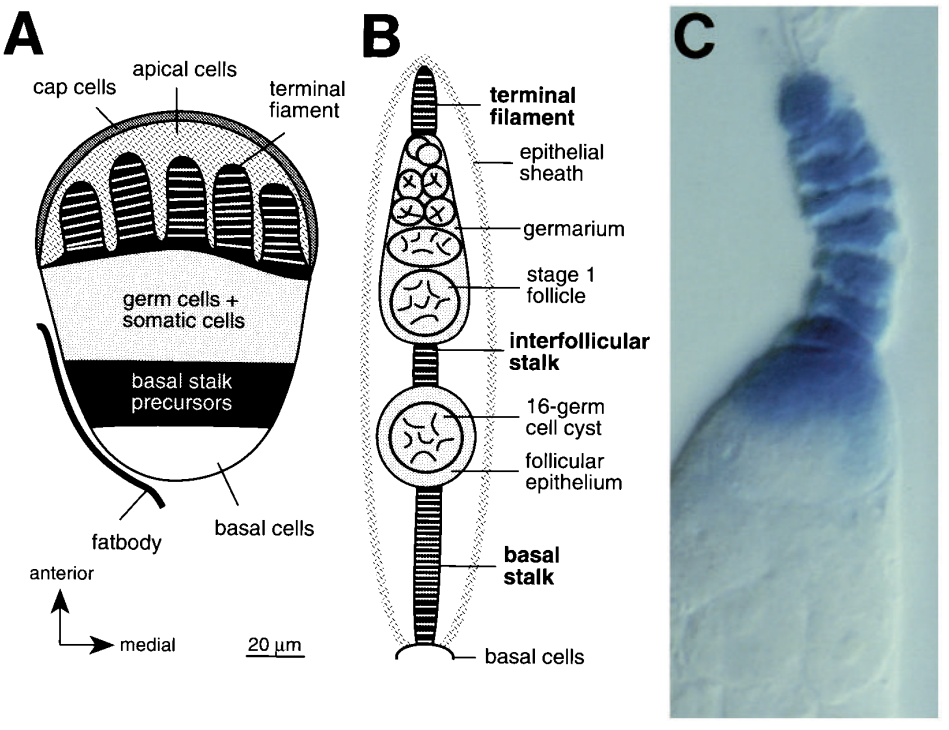

Fig. 1. A diagram of (A) a wild-type ovary at puparium formation and (B) an ovariole 2.5 days afterwards. (C) An adult terminal filament with eight disc-shaped cells that express β-gal in females of the *bab*^{A128} enhancer trap line.

to the eye-shaped appearance of the clusters. The bundling is accompanied by a strong accumulation of actin filaments in these ends where the cells from adjacent clusters contact each other (Fig. 4C). The cells of individual stacks remain elongated and bundled while new TF cells are added posteriorly to the stack (Fig. 4D). These additional TF cells also intercalate and sort out when they join a particular cluster. When complete TF cell clusters of 8-9 cells have formed, the apical cells begin their migration between the TFs (stage 3; Fig. 4D). The transformation from the eye-shaped clusters into mature TFs occurs when the TFs become separated from each other by the invading apical cells. At this time the TF cells change from a spindle shape into a disc shape with a blunt margin all around their circumference (stage 4; Fig. 4E). Actin filaments remain concentrated along the margins. Our results suggest that cell intercalation is the driving force in the formation of distinct TF cell clusters along the dorsal-ventral axis. In contrast, there appears to be no overlap of cells between successively emerging TF clusters along the medial-lateral axis. Even small clusters are clearly separated from each other along this axis (Fig. 4A).

The strong bundling of the TF cells and the striking actin filament distribution suggests that the tapered ends of the TF cells may be highly adhesive to each other. To investigate this possibility, we have examined the distribution of Armadillo (Arm) protein during TF formation. Arm is closely related to the vertebrate β-catenin and plakoglobin and is a component of cell-cell adherens junctions (Peifer and Wieschaus, 1990; Peifer, 1993). Most of the Arm protein is seen along the cell membranes in anti-Arm-stained larval ovaries. In an eye-shaped TF the Arm protein is found in spots along the whole surface of the TF cells but is concentrated at the tapered ends of the TF cells like the actin filaments (Fig. 5A). Interestingly, the protein becomes redistributed when a mature TF forms. Arm is still found along the membranes between the TF cells but its concentration along the margins is drastically reduced (Fig. 5B).

Terminal filaments are polyclonal in origin

During the development of a TF, its cell number increases gradually. This raises the question whether the 8-9 cells of a stack derive from a single precursor cell or whether TFs form by cell recruitment. Our morphological analysis suggests that cell rearrangement is involved in TF development which is consistent with a polyclonal origin for the cells of a TF. A genetic mosaic experiment was performed to test this hypothesis. Clones in the TFs were created by somatic recombination with the yeast FLP recombinase-FRT system (Golic, 1991; see Material and methods). The clones were genetically labeled using the TF cell marker *bab*^{A128}, a P[*lacZ*] insertion mutation that does not cause defects in ovary development. Cells of mosaic patches contain zero copies (unlabeled cells) and two copies of *lacZ*.

24 mosaic ovaries were examined, each deriving from a somatic recombination event in the early second larval instar, a day before onset of TF formation (Table 1). Two observations were made. First, the mosaic ovaries contain stacks where

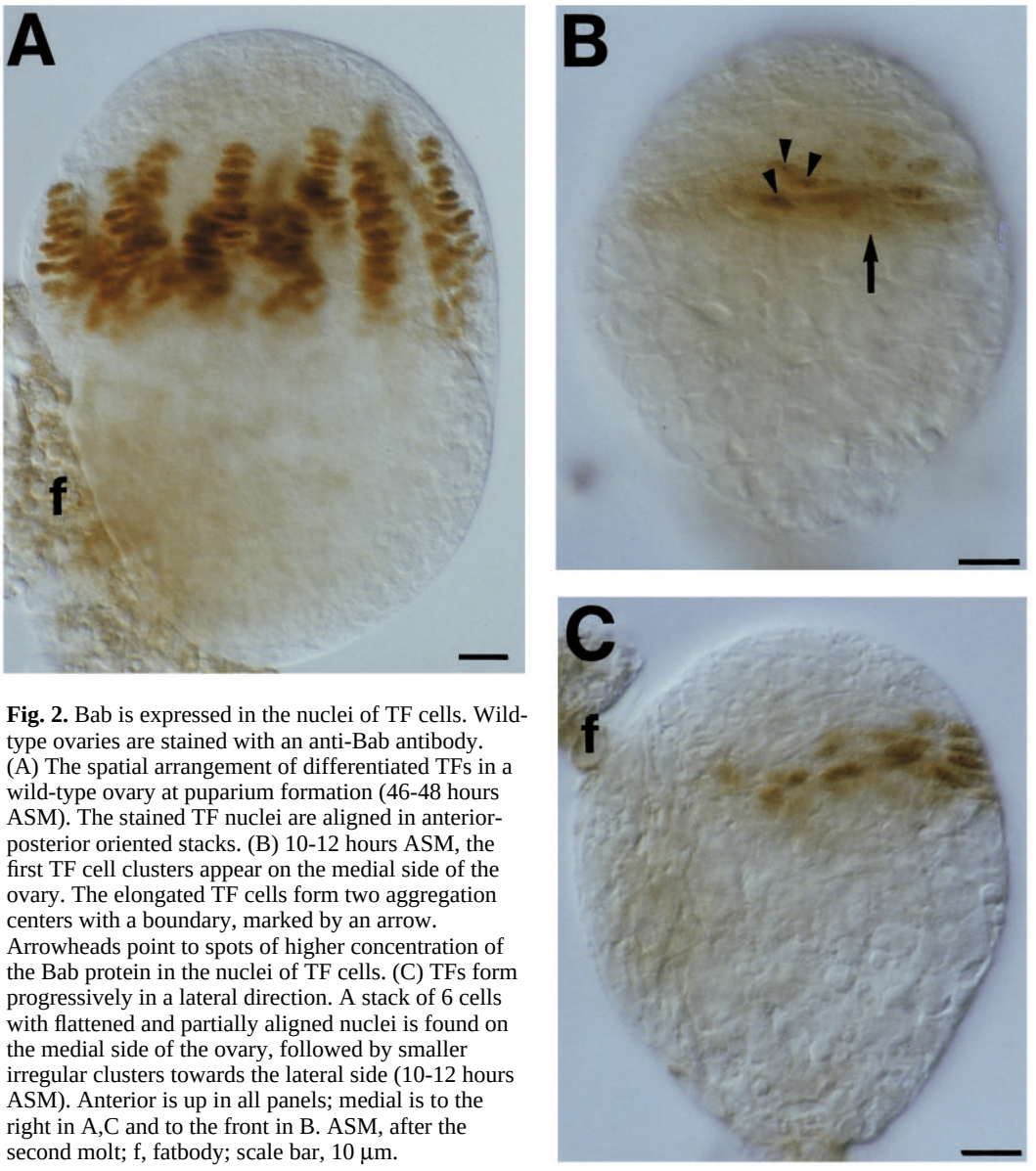

Fig. 2. Bab is expressed in the nuclei of TF cells. Wild-type ovaries are stained with an anti-Bab antibody. (A) The spatial arrangement of differentiated TFs in a wild-type ovary at puparium formation (46-48 hours ASM). The stained TF nuclei are aligned in anterior-posterior oriented stacks. (B) 10-12 hours ASM, the first TF cell clusters appear on the medial side of the ovary. The elongated TF cells form two aggregation centers with a boundary, marked by an arrow. Arrowheads point to spots of higher concentration of the Bab protein in the nuclei of TF cells. (C) TFs form progressively in a lateral direction. A stack of 6 cells with flattened and partially aligned nuclei is found on the medial side of the ovary, followed by smaller irregular clusters towards the lateral side (10-12 hours ASM). Anterior is up in all panels; medial is to the right in A,C and to the front in B. ASM, after the second molt; f, fatbody; scale bar, 10 μm.

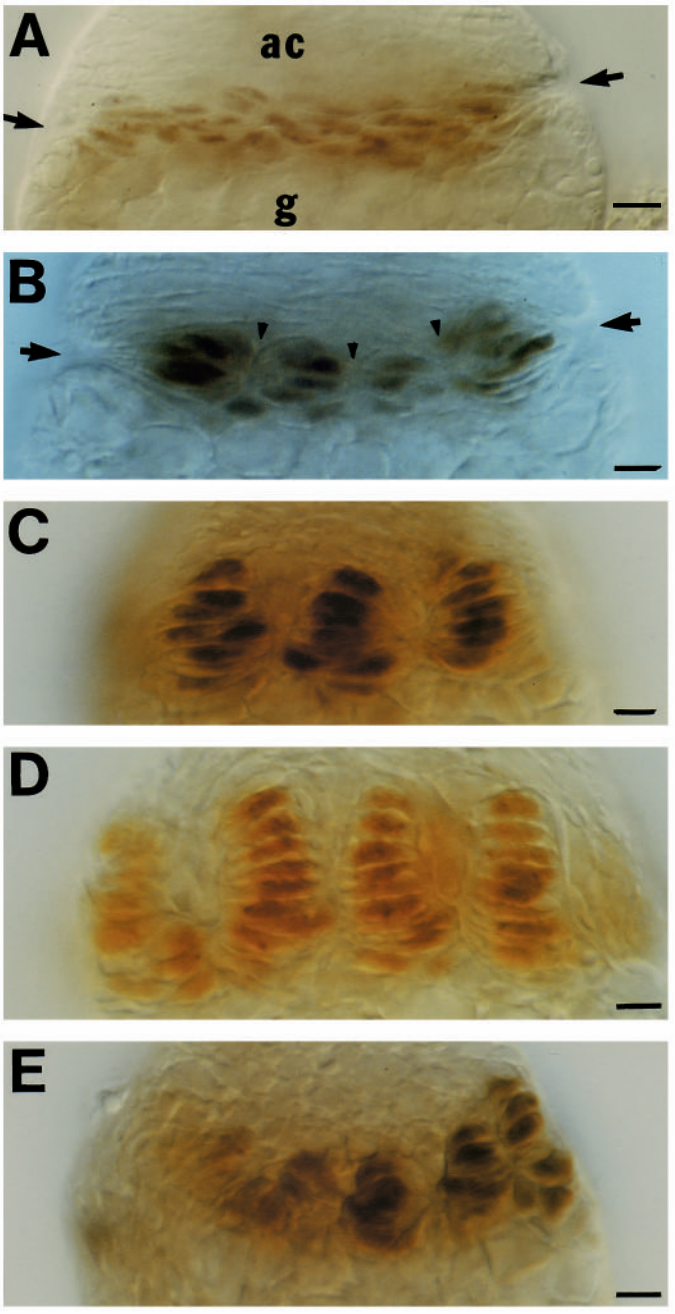

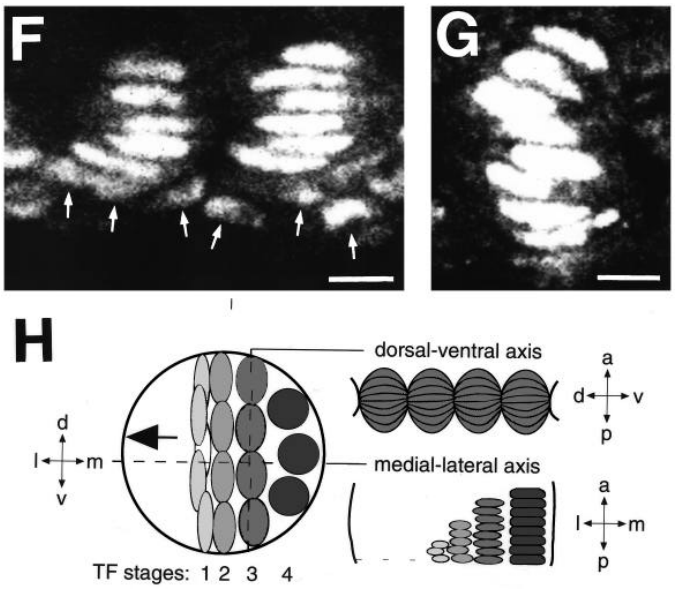

Fig. 3. Formation of TFs. TF cell nuclei are visualized with an anti-Bab antibody using Nomarski (A-E) or confocal optics (F,G). (A-D) The different stages in TF development in third larval instar ovaries. (A) Stage 1. The spindle-shaped TF cells are uniformly distributed in a layer between the apical cells (anterior) and the germ cells (posterior). A furrow is found on the surface of the ovary in the TF region (arrow). (B) At early stage 2 eye-shaped clusters of TF cells have formed. TF cell nuclei are not aligned. Boundaries between clusters are marked with an arrowhead, the ovary furrow with an arrow. (C) Stage 3 eye-shaped clusters with increased cell number (medial side of an ovary at 25-27 hours ASM). (D) Stage 4. Mature TFs with disc-shaped cells and aligned nuclei (medial side of an ovary at 32-34 hours ASM). (E) Same ovary as in (C; turned by 90°) which shows the developmental gradient of TFs along the medial-lateral axis. The number of cells per stack decreases from medial to lateral. TF cells are stretched out along the dorsal ventral axis (see C) and are narrow along the medial-lateral axis. (F) Weakly stained nuclei (arrows) are located posteriorly to clusters with strongly stained and almost aligned nuclei (late stage 2). (G) A TF cell cluster after additional cells are integrated into the stack (stage 3). (H) Schematic drawings of TF formation in different perspectives. TFs develop simultaneously along the dorsal-ventral axis and progressively along the medial-lateral axis. The large arrow indicates the direction in which TFs consecutively form; the thick lines indicate the surface of the ovary. Anterior is up in panels A-G; medial is to the right in E and to the front in panels A-D,F,G. ASM, after the second molt; g, germ cells; ac, apical cells; a, anterior; p, posterior; m, medial; l, lateral; d, dorsal; v, ventral; scale bar, 5 μm.

stained and unstained TF cells are mixed (Fig. 6A,E). The distribution pattern of stained and unstained stacks is different from stack to stack and appears random. Second, unstained cells are distributed over several TFs in all the mosaic ovaries (Fig. 6A,E). The mosaic stacks of an ovary are not scattered but lie together in a group. Because the frequency of mosaic ovaries is relatively low in this sample (see Table 1), we estimate that in approximately 85% of the mosaic ovaries all the unstained cells derive from a single mitotic recombination event (see Material and methods). This indicates that cells from a single clone are distributed between different TF stacks. Both observations show that TFs are of polyclonal origin and suggest that TFs form by a cell recruitment mechanism. Furthermore, this experiment allows an estimate of the number of TF progenitor cells at the early second larval instar. Taking into account an average number of 164 TF cells per ovary (20 ovarioles with about 8 TF cells each) and 10-18% unstained cells in a mosaic ovary (8 mosaic ovaries evaluated), an induced clone (all cells with either 0 or 2 copies of *lacZ*) occupies a fifth to a third of the TF territory. This suggests that there exist 3-5 TF progenitor cells in the early second larval instar.

Clones are produced at higher frequency by heat shock at early third larval instar when TFs start to form and at mid third larval instar when TF formation is fully in progress. In a control experiment where the FLP gene was absent, mosaic ovaries were not detected (Table 1). The position of a labeled clone in a mosaic ovary depends on the time point of mitotic

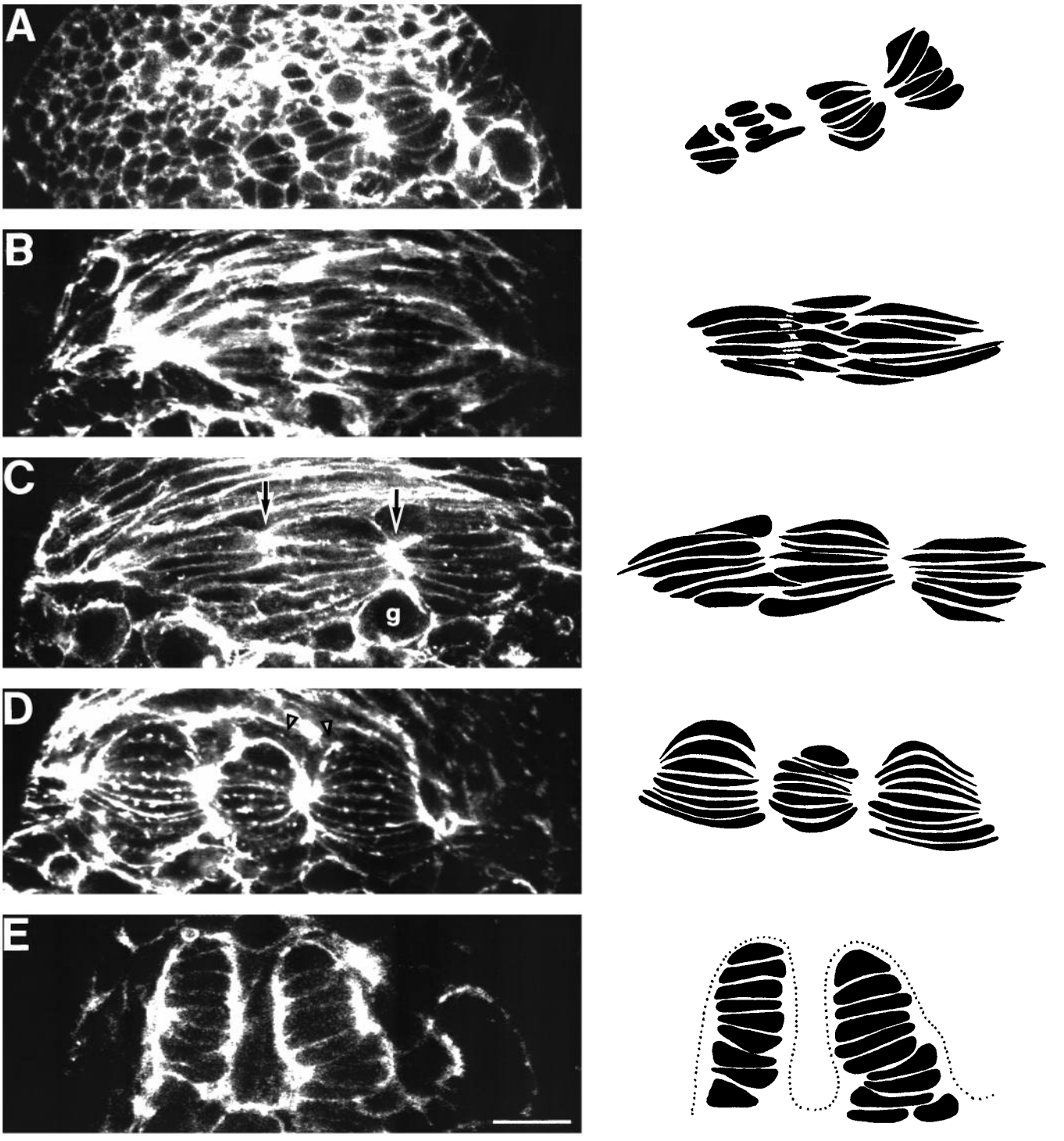

recombination. In mosaic ovaries induced at early third larval instar, clonal cells are primarily found in stacks on the medial side of the ovary or extending from medial to lateral (14 out of 18 mosaic ovaries). In contrast, clones induced during mid third larval instar were found predominantly located on the very lateral side of the ovary (11 out of 16 mosaic ovaries; Fig. 6C,D). The difference in the location of early and mid third larval instar induced clonal cells apparently reflects the developmental gradient in TF formation. Mosaic ovaries produced at third larval instar, like at second larval instar, contain TFs consisting of stained and unstained cells. Because of the high frequency of mosaic ovaries induced at third larval instar, the unstained cells likely correspond to multiple recombination events. The late-induced clones indicate that the gradual development of a TF is based on a sequential recruitment of TF cells, which do not come from a large preformed cell pool but rather from TF precursor cells that continue to divide in parallel to the process of TF formation.

Fig. 4. Distribution of actin filaments during TF formation. Confocal images of phalloidin stained wild-type ovaries accompanied by an illustration showing shape and position of the TF cells at the different stages of TF formation. (A) Progressively forming TFs along the medial-lateral axis at mid third larval instar. Four non overlapping stacks are visible. The cells of the two medially located stacks are wider than of the cells of the lateral stacks. Cells located laterally to the TF stacks and all the anterior located cells (apical cells) have a small round outline in this view. (B-E) Formation of distinct TF cell clusters along the dorsal-ventral axis. TFs form in a layer between the apical cells (anterior) and the germ cells (posterior). (B) TF cells and the apical cells are extremely elongated. The TF cells of two prospective stacks are intercalated (stage 2). (C) Three clusters in a row (stage 2). Anterior TF cells of the left and the middle stack have separated while the posterior TF cells are still interdigitated. A separate stack is seen to the right. As distinct eye-shaped clusters form actin filaments become concentrated in the tapered ends of the TF cells (arrows). The apical cells form a separated layer anterior to the TF cell clusters (D). Three distinct eye-shaped clusters containing the final number of TF cells (stage 3). Actin filaments are concentrated in the spindle-shaped TF cells at the contact sites between the stacks. An arrowhead points to apical cells which have changed the orientation of their longitudinal axis and move between the TFs. (E) Two mature TFs which are separated by migrating apical cells (stage 4). TF cells have become disc-shaped. The tapered ends have turned blunt forming now the tissue boundary where the actin filaments remain concentrated. Anterior is up in all panels; medial is to the right in A and to the front in B-E. g, germ cell; scale bar, 10 μm.

Basal stalks and interfollicular stalks form by cell intercalation

BSs and the first IFSs appear in the ovary during the pupal stage. The expression of Fasciclin III on the surface of IFS cells (Brower et al., 1981) and BS cells was used to follow their development. At the end of the third larval instar, the BS primordium is located between the germ cells and the basal cell population (Figs 1A, 11E). When the apical cells that will form the epithelial sheaths migrate from anterior to posterior during the first day after puparium formation, they subdivide the germ cells as well as BS cells into small subpopulations, and a thick basement membrane (tunica propria) is laid down at the interface of the intruding apical cells and the enclosed cells (King, 1970). The BS cells have a rounded cell shape during this period (Fig. 7C), and their cell number increases (data not shown). During the second day after puparium formation, the BS subpopulations, each about three cell diameters wide, transform into long stalks, each only one cell diameter wide (Fig. 7). The narrowing and elongation of the BS primordia is accompanied by striking changes in the shape of the BS cells. The BS cells flatten, in the same direction (anterior-posterior) into which the whole cell population extends (Fig. 7D). BS cells apparently intercalate with each other. Cells along the tissue boundary are wedge-shaped during this morphogenetic process (Fig. 7E), with the blunt side contacting the basement membrane. At the end of the process, the BS cells are surrounded by basement membrane along its whole circumference and they become disc-shaped (Fig. 7F). The BS is only a transient structure and begins to degenerate during the third day after puparium formation.

IFSs connect the follicles of an ovariole and appear as soon as follicles separate from the germarium, a process that starts about 2.5 days after puparium formation and continues through the adult life. When IFS cells become recognizable as a distinct cell group between the germarium and a budded follicle, they form a short and thick stalk (Fig. 8A). Similar to BS development, intercalation of the wedge-shaped IFS cells and a subsequent change in cell shape leads to the formation of a single

Table 1. Mosaic analysis of terminal filaments

Cross (females × males)*	Larval stage at time of heatshock	Mosaic ovaries/ total no. of ovaries†	Mosaic ovaries [%]‡
bab^{A128} FRT2A × *FLP/+; FRT2A/+*	early 2nd	7/146 3/80 14/300	18§
bab^{A128} FRT2A × *FLP/+; FRT2A/+*	early 3rd	10/75 8/67	51§
bab^{A128} FRT2A × *FLP/+; FRT2A/+*	mid 3rd	16/86	74
bab^{A128} FRT2A × *FRT2A* (control)	early 3rd	0/97	–

**P[lacZ]* enhancer detector *bab^{A128}* is used as a genetic marker for terminal filament cells.

†Repeated experiments are listed separately.

‡Percentage is related to the 25% ovaries expected to have the genotype *FLP/+; bab^{A128} FRT2A/ + FRT2A* that allows mitotic recombination.

§Average percentage for repeated experiments is given.

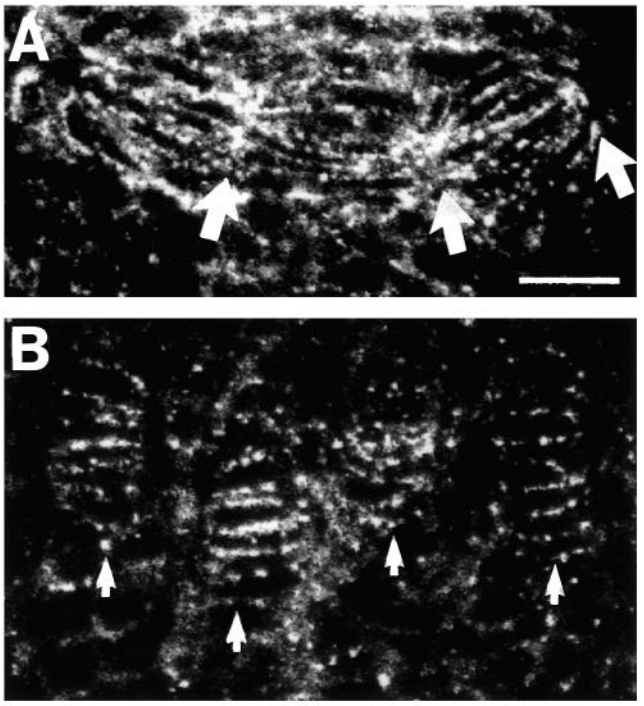

Fig. 5. Distribution of Arm during TF formation. Confocal images of anti-Arm-stained wild-type ovaries. (A) In the three eye-shaped TF cell clusters Arm is found in spots along the cell membranes and is highly concentrated in the tapered ends of the cells where neighboring stacks are in contact (arrows). (B) In mature TFs (arrows point to four stacks) Arm is found in spots along the anterior and posterior membranes of cells in a stack. By contrast, the blunt margins of the cells show little staining. Anterior is up in all panels. Scale bar, 10 μm.

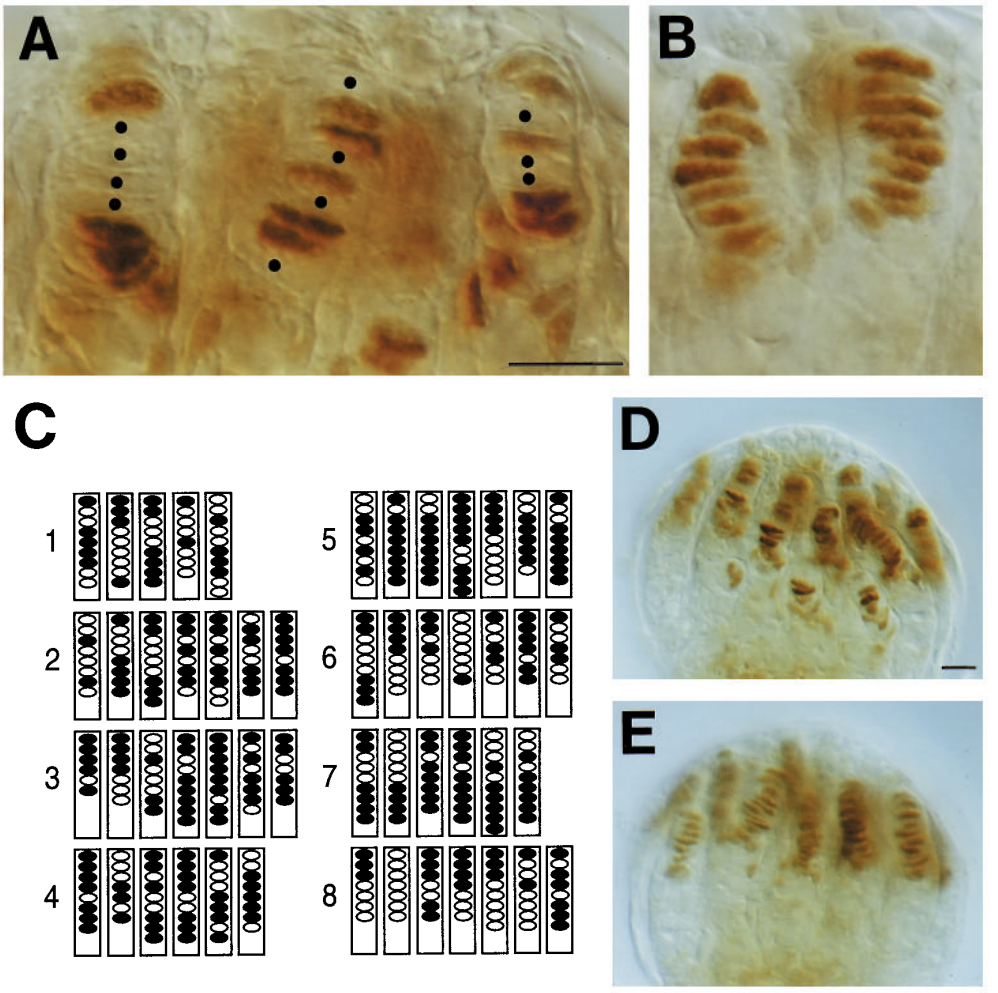

Fig. 6. Clonal analysis of TFs. In the experiment (see Material and methods), 25% of the larvae are expected to have the genotype that enables mitotic recombination and the production of twin clones, one which lacks the P[*lacZ*] insert and one that has two copies of the insert. The examination is based on the distribution pattern of the cells that lack the insert and therefore are unlabeled in an anti-β-gal assay (Cells containing one or two *lacZ* copies could not always be distinguished based on staining intensity using the bab^{A128} enhancer trap line). (A) Three mosaic TFs which derived from a mitotic recombination event in an early second instar larva. The order of stained and unstained cell nuclei is different from stack to stack. All unstained cells (marked by dots) presumably belong to a single clone. (B) An example of non-mosaic stacks. (C) A diagram of the mosaic TFs from eight ovaries produced by mitotic recombination in the early second larval instar (the non-mosaic TFs are not shown). Some stacks show less than the normal cell number because unstained cells at the bottom or top of a stack could not always be clearly identified. (D) A view of the lateral side of an ovary where mosaic stacks are located and (E) of the medial side of the same ovary which contains non-mosaic TFs. Strongly stained cells in mosaic stacks are probably the twin clones to the unstained cell clones and have two copies of the reporter gene. Mitotic recombination in E was induced at mid third larval instar. Anterior is always up. Scale bar, 10 μm.

row of disc-shaped cells (Fig. 8B,C). A group of BS or IFS cells that will give rise to a single stalk is already enclosed by epithelial sheath cells prior to stalk formation. This suggests that the individual BSs or IFSs develop independently from each other, in contrast to the formation of TFs, where multiple stacks develop from an undivided common cell population.

bab mutant ovaries lack ovarioles

Mutations in the gene *bab* cause a mutant phenotype in legs (Godt et al., 1993) and in ovaries. *bab* mutant females are sterile and have ovaries of an aberrant morphology (Fig. 9). In comparison to the cone-shaped wild-type adult ovary, the *bab* mutant ovary is very small and abnormally shaped. Ovaries that are homozygous for strong hypomorphic alleles, such as bab^{PRDS}, bab^{PR24} and bab^{PR72}, which do not express the Bab protein at a detectable level, have a severely reduced ovariole number or lack ovarioles altogether. A dominant haploinsufficient effect of *bab* mutations, previously described for legs, has not been observed for ovaries. The *bab* mutant adult ovary phenotype is complex. This study analyzes the requirement of *bab* on the development of TFs, BSs and IFSs. Additional aspects of the *bab* mutant phenotype will be described elsewhere (Sahut, Godt, Laski and Couderc, unpublished data).

bab mutations disrupt the formation of terminal filaments

Ovary defects in *bab* mutants are first detected in the third larval instar. Wild-type ovaries take on an oval shape when the TFs develop. In contrast, *bab* mutant ovaries maintain a nearly round shape, and analysis shows that TFs fail to form. Enhancer traps that express *lacZ* in TFs were used to study the *bab* mutant ovary phenotype. These included the strong allele bab^{PRDS}, as well as AD47, XA42 and B1-93F, which map to other loci and which were used in the background of the β-gal negative bab^{PR24} and bab^{PR72} mutations. The analysis shows that TF cells are affected in a strong hypomorphic *bab* mutant to a variable degree (Fig. 10A,B,C). (1) The number of cells that express the four TF markers is severely reduced in the TF region as compared to wild-type. (2) Most of these cells have aberrant morphogenetic properties. They have a rounded cell shape and form loose aggregates that do not differentiate into stacks. (3) A very few TF cells have a flattened cell shape and form short and irregular stacks of 2-5 cells. This probably reflects some residual *bab* activity in the examined *bab* mutants; however, study of *bab* null alleles will be necessary to exclude the possibility that TF formation is to a minor degree independent of *bab* function. (4) bab^{PRDS} hemizygous ovaries

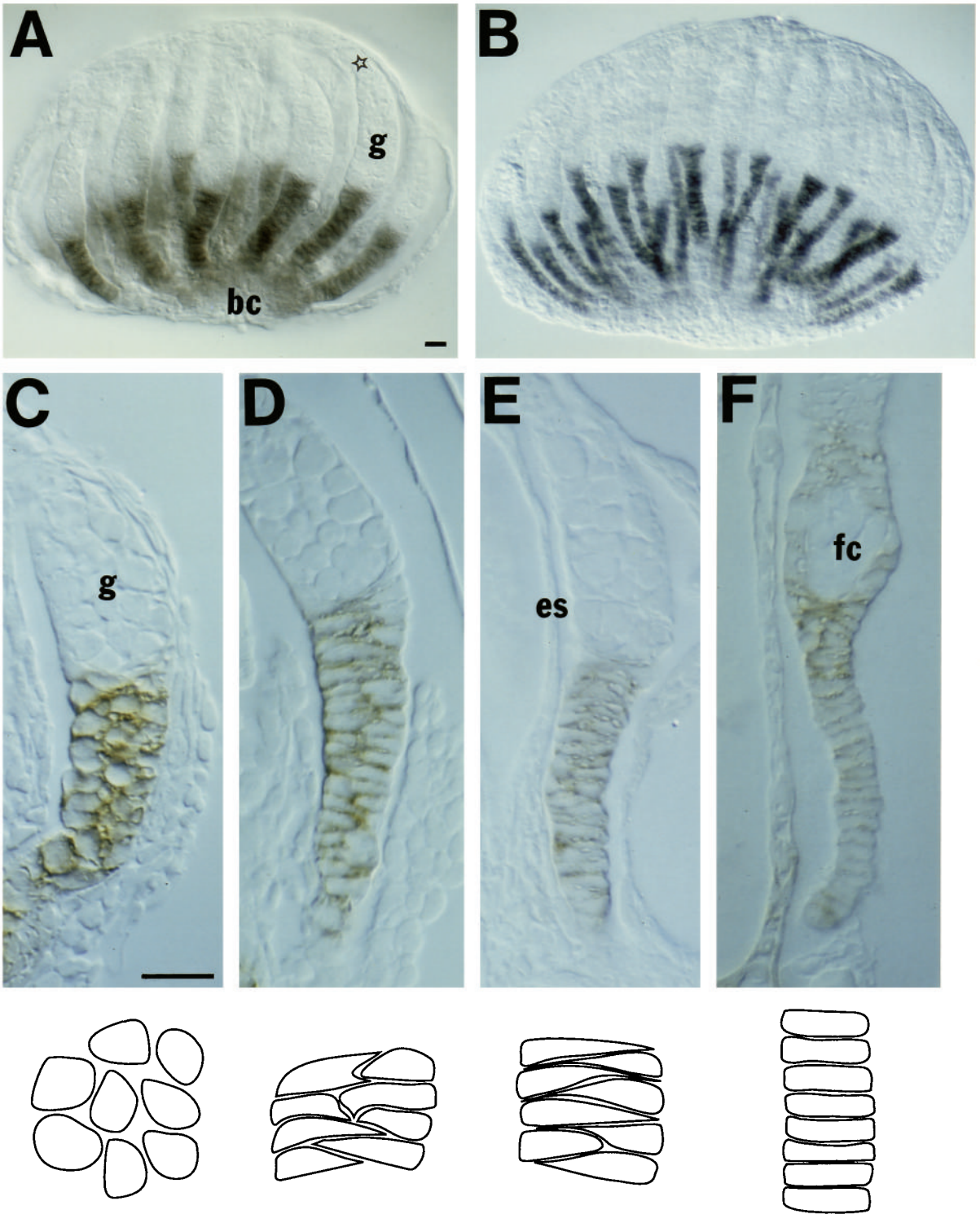

Fig. 7. BS formation in wild-type pupal ovaries. The surface of BS cells is stained with an anti-Fasciclin III antibody. (A,B) Whole-mount ovaries showing the transition from short and thick BS primordia into long and thin BSs which occurs around 40 hours APF. The BS connects the germarium to the basal cell population. A TF is marked by a star. (C-F) Sections of ovarioles during different stages of BS development accompanied by a drawing of a group of BS cells. (C) 16 hours APF the BS primordium is about three cell diameters wide and the BS cells are round. (D) 40 hours APF the BS is two cell diameters wide and cells have flattened and intercalate between each other. (E) Briefly afterwards wedge-shaped BS cells are organized in a single row. (F) A mature BS with disc-shaped cells. 64 hours APF the stalk is already detached from the basal cells and shortened. Anterior is up in all panels. APF, after puparium formation; g, germarium; bc, basal cell population; es, epithelial sheath; fc, follicle; scale bar, 10 μm.

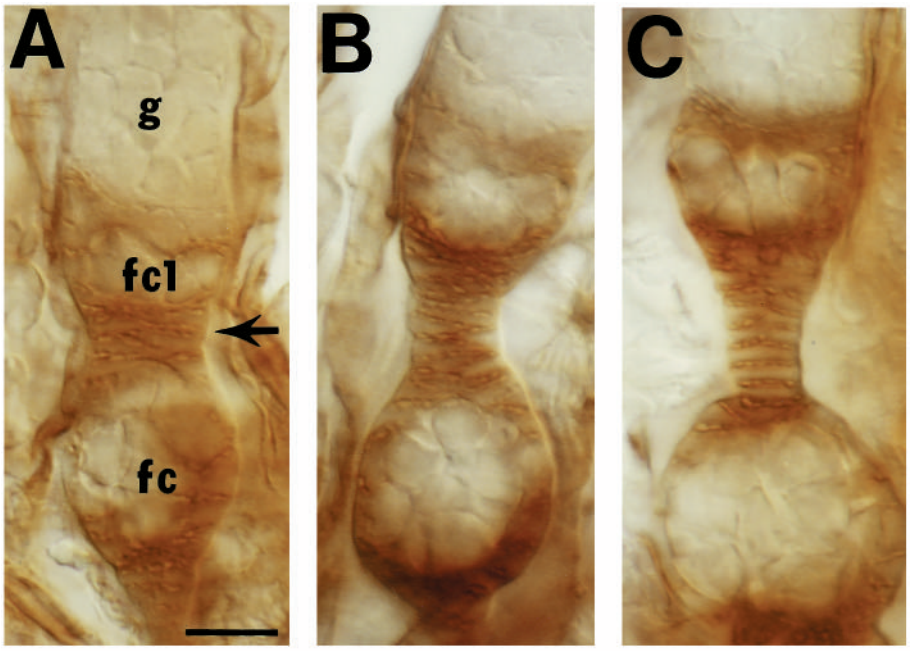

Fig. 8. IFS formation in wild-type ovaries. The surface of IFS cells and follicle cells is labeled with an anti-Fasciclin III antibody. (A-C) Consecutive stages in the formation of an IFS (arrow) between a stage 1 follicle (fc1) in the germarium (g) and a budded follicle (fc) in a pupal ovariole. Intercalation of the wedge-shaped IFS cells and a change in cell shape lead to a stalk of disc-shaped cells. Anterior is up in all panels. Scale bar, 10 μm.

have cells in the posterior region that express *lacZ*, which is not seen in *bab*^{PRDS} heterozygous ovaries (Fig. 10A,B). These cells show a lower staining level than the anterior cells, have a rounded shape and show signs of degeneration. Because the posterior cells also express a TF marker unrelated to *bab* (B1-93F; Fig. 10C) the simplest assumption is that these are TF cells that are misplaced due to cellular defects which would also explain the strongly reduced number of TF cells in the anterior region. Alternatively, TF-specific genes might be ectopically expressed in another cell population in *bab* mutant ovaries and the reduced number of TF cells might be due to cell death or an altered cell fate.

bab is required cell autonomously for terminal filament development

To study whether *bab* is autonomously required in TF cells, a

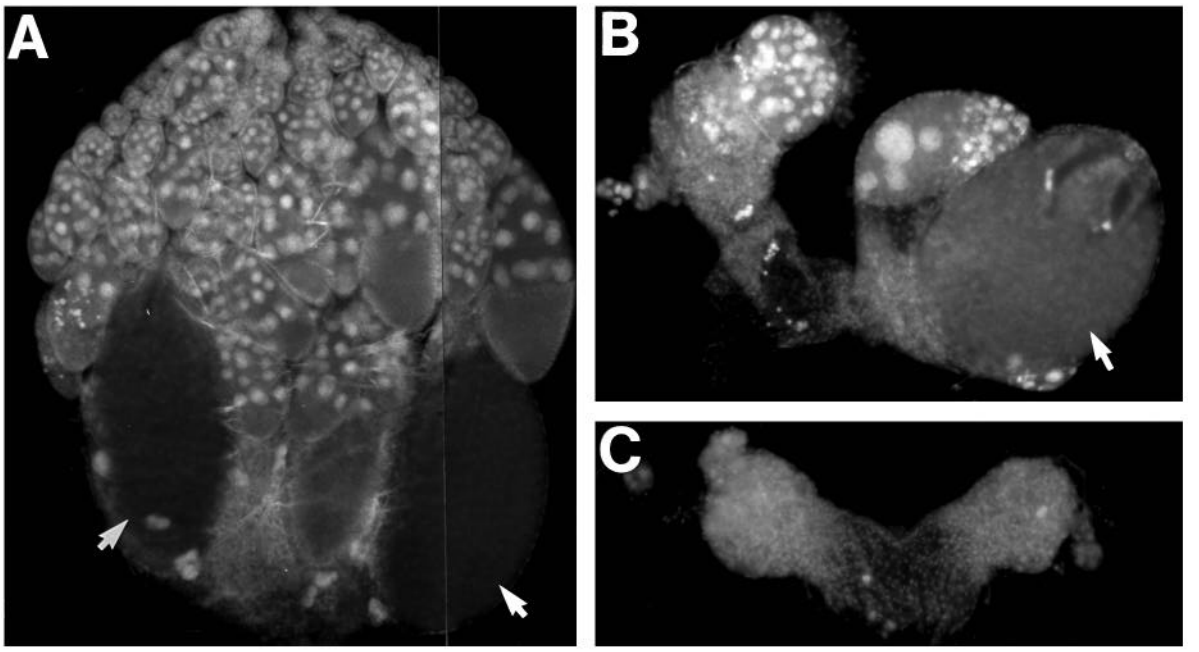

Fig. 9. The adult *bab* mutant ovary phenotype. Cell nuclei are visualized by DAPI staining. (A) The wild-type ovary has approximately 20 ovarioles which are oriented in parallel and contain a series of follicles of advancing developmental stages from anterior to posterior. The large polyploid cell nuclei of the nurse cells are stained intensely. (B-C) A pair of *bab*^{PRDS} homozygous ovaries, which are connected by an oviduct (same magnification as in A). (B) Both ovaries contain a rudimentary ovariole with a few follicles. (C) The ovaries do not contain any follicles. Anterior is up in all panels. Arrows point to mature oocytes.

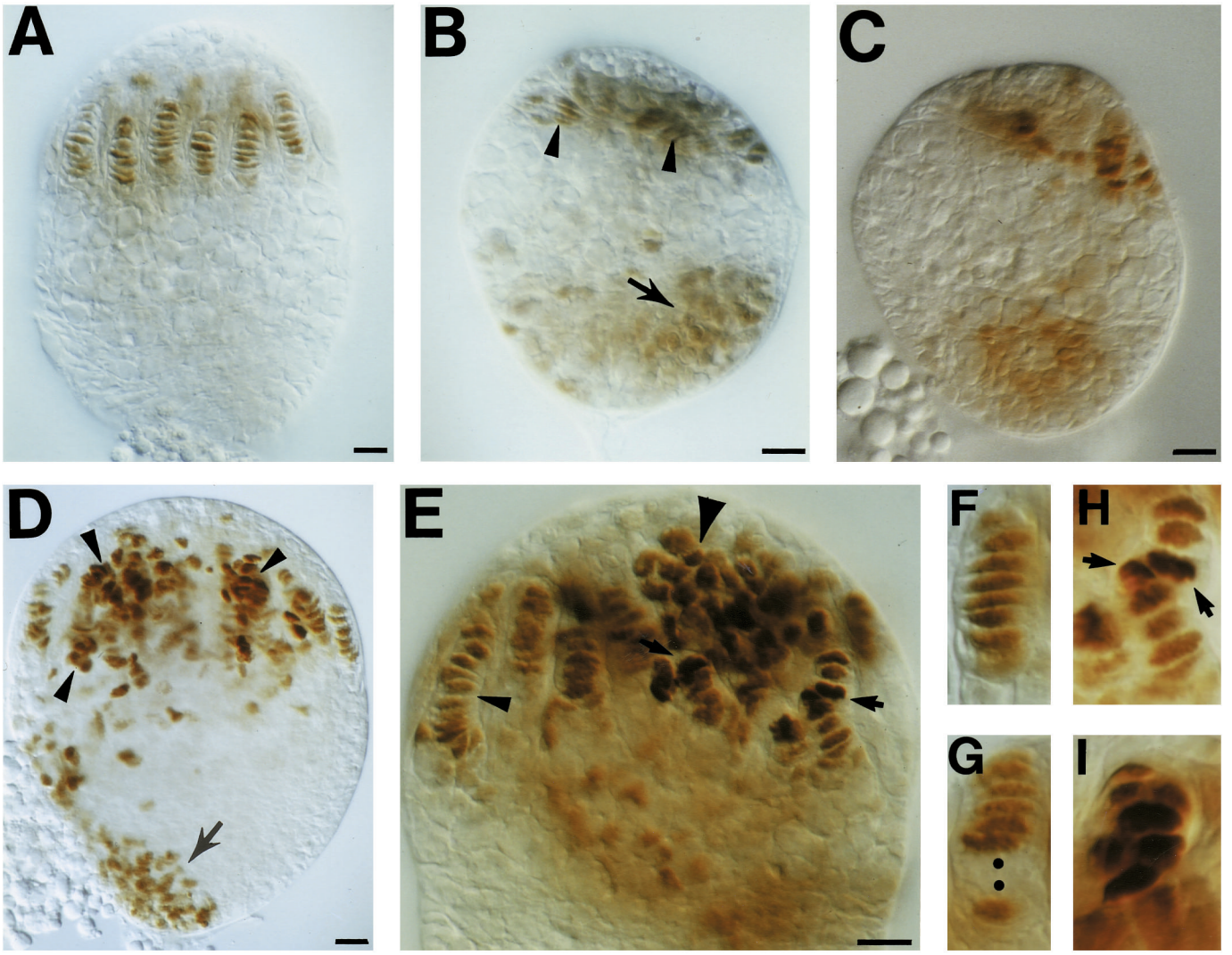

Fig. 10. *bab* mutations disrupt the formation of TFs in the ovary. Ovaries from white prepupae are stained with an anti-β-gal antibody. (A) A bab^{PRDS}/+ ovary has normal TFs. β-gal is localized in the nuclei of the TF cells. (B) In a bab^{PRDS}/*Df(3L)*bab^{PG} ovary, TFs have not formed and the ovary has an abnormal shape. Some of the strongly stained cells in the anterior region have a flattened nucleus (arrowhead), typical for TF cells. In addition, a group of stained cells is found posteriorly in the ovary (arrow). (C) The enhancer trap insertion B1-93F, which expresses *lacZ* only in TF cells in a wild-type ovary (not shown), expresses *lacZ* in the anterior and posterior region of a bab^{PR24} homozygous ovary similar to the staining pattern of the ovary seen in panel (B). (D-I) TF mosaic analysis for the bab^{PRDS} mutation. Mitotic recombination was induced in the early second larval instar. (D) Strongly stained bab^{PRDS} homozygous mutant cells are scattered throughout the TF region or are located in small irregular clusters (arrowheads). A number of stained cells is also found in the posterior region of the ovary (arrow). (E) TF region of a mosaic ovary. Weakly stained cells have formed normal TFs (small arrowhead). Most of the strongly stained *bab* mutant cells are found in a large loose aggregate and have a rounded nucleus (large arrowhead). A few darkly stained *bab* mutant cells participate in stack formation (arrows). (F-I) Single stacks of mosaic ovaries at higher magnification. (F) Single normal stack of weakly stained *bab* heterozygous cells. (G) Single mosaic stack with weakly stained *bab* heterozygous cells and unstained wild-type cells (marked by dots) that lost the *bab* mutation due to mitotic recombination. (H) Single mosaic stack that contains two *bab* mutant cells (arrow) which are not properly aligned with the *bab* heterozygous cells. (I) Mosaic cell aggregate where *bab* heterozygous and homozygous mutant cells have not aligned into a single row. Scale bar, 10 μm.

mosaic analysis was conducted using the strong allele bab^{PRDS} which also serves as a TF cell marker (see Material and methods). bab^{PRDS} homozygous cells stain detectably stronger in an anti-β-gal assay than heterozygous cells and can therefore be easily identified. Clones were induced at early or mid second or early third larval instar, and 11, 58, and 15 mosaic ovaries were recovered, respectively. Unstained cells, which lost the marker and are wild type, and light-colored heterozygous cells have a flattened shape and form normal TFs in the mosaic ovaries (Fig. 10D-G). Most of the darker stained *bab* mutant cells have a rounded cell nucleus, are scattered or form loose aggregates in the TF region, but do not form normal stacks (Fig. 10D,E,I). Occasionally, dark stained cells were found integrated into a TF. This finding is not surprising because in non-mosaic *bab* mutant ovaries a few TF cells form rudimentary stacks. Interestingly, the alignment of TF cells in

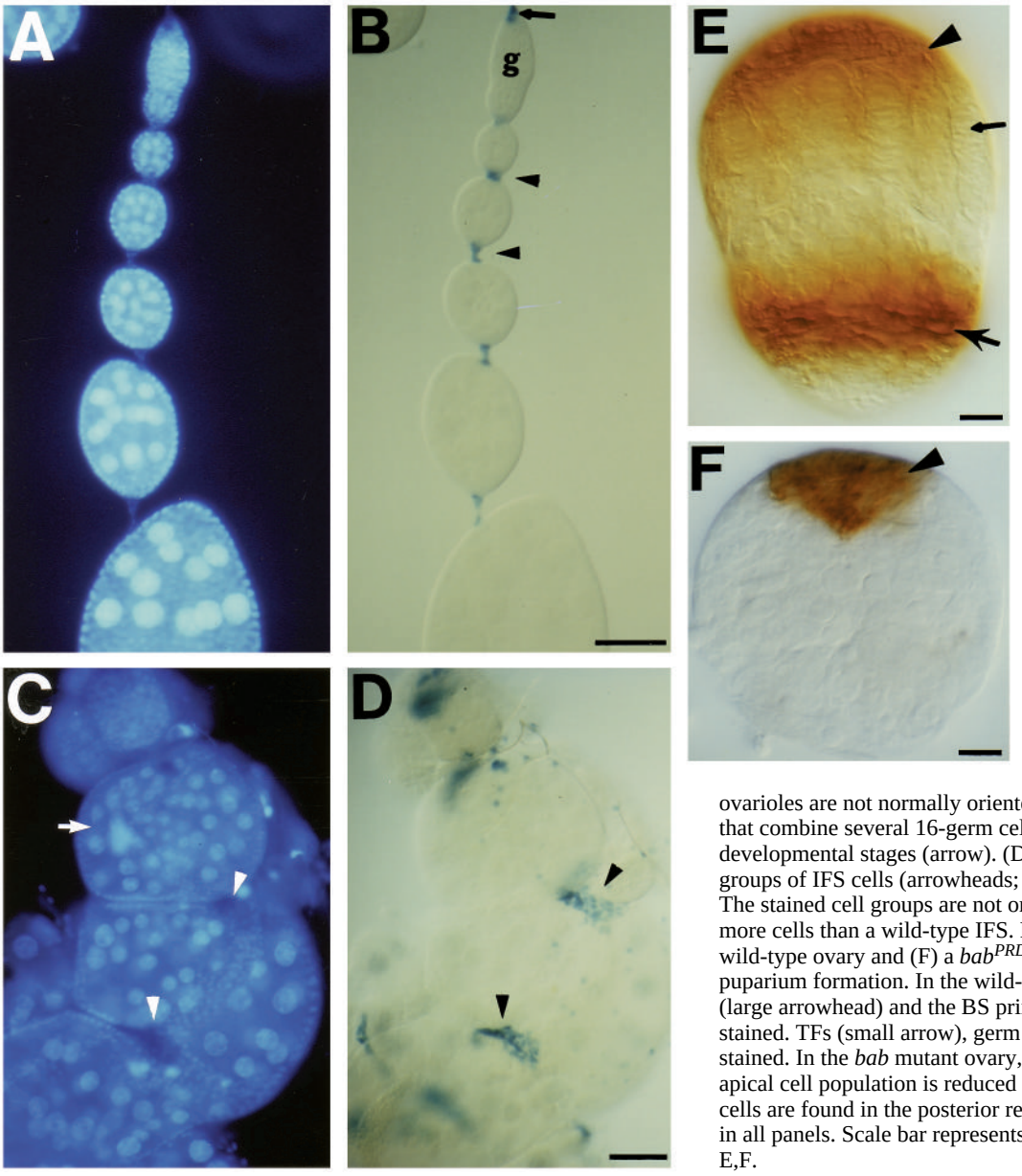

Fig. 11. BSs and IFSs are affected in *bab* mutant ovaries. (A,C) Visualization of cell nuclei by DAPI staining and (B,D) detection of the IFSs in adult ovaries by X-gal staining using the enhancer detector B1-93F. (A,B) The same wild-type ovariole with the TF at the anterior end (arrow), followed posteriorly by a germarium (g) and a number of follicles that are connected by IFSs (arrowheads). Each follicle contains a 16-germ cell cyst which is surrounded by a follicular epithelium. (C) In a bab^{PR72} homozygous ovary, the remaining ovarioles are not normally oriented and contain fused follicles that combine several 16-germ cell cysts of different developmental stages (arrow). (D) The follicles are connected by groups of IFS cells (arrowheads; seen as dark areas in panel C). The stained cell groups are not organized into stacks and contain more cells than a wild-type IFS. Fasciclin III staining of (E) a wild-type ovary and (F) a bab^{PRDS} homozygous ovary at puparium formation. In the wild-type ovary, the apical cells (large arrowhead) and the BS primordium (large arrow) are stained. TFs (small arrow), germ cells and basal cells are not stained. In the *bab* mutant ovary, TFs are not apparent and the apical cell population is reduced in size. No Fasciclin III-positive cells are found in the posterior region of the ovary. Anterior is up in all panels. Scale bar represents 50 μm in A-D and 10 μm in E,F.

a mosaic stack is disturbed at the point where a mutant cell is located, which can lead to a kink in the TF (Fig. 10E,H). Furthermore, the mosaic ovaries contain in addition to the mutant cells in the TF region *lacZ* expressing cells ectopically in a more posterior region of the ovary similar to non-mosaic *bab* mutant ovaries (Fig. 10D). These observations show that *bab* mutant TF cells display autonomously aberrant morphogenetic features.

bab mutations affect the development of basal stalks and interfollicular stalks

Disruption of TF formation is the earliest defect observed in *bab* mutant ovaries. Subsequently, defects develop involving other somatic cell populations. Staining with anti-Fasciclin III reveals defects in the BS primordium from puparium formation onwards. In wild type, Fasciclin III is expressed in the BS primordium and the apical cell population at puparium formation (Brower et al., 1980 and 1981; Fig. 11E). In strong *bab* mutant ovaries, no cells or only a small number of cells are stained in the BS region and the stained apical population is strongly reduced in size, which causes the remaining TF cells to be located more anteriorly than in wild type (Fig. 11F). Increased cell death is observed in both regions (data not shown).

In wild-type adult ovarioles, the follicles are separated from each other by interfollicular stalks (Fig. 11A,B). The remaining ovarioles in *bab* mutant adult ovaries contain follicles of different developmental stages, which are partially or completely fused and of irregular shape (Fig. 11C). To identify IFS cells in the disorganized ovaries of *bab* mutants, the enhancer trap B1-93F was used as a genetic marker (Ruohola et al., 1991; Fig. 11D). Stained cells are found between adjacent follicles of *bab* mutant ovarioles. These cells however, are not aligned in a single row but are organized as an irregular band (Fig. 11C,D). The larger number of β-gal-positive cells per cluster, as compared to a wild-type IFS, seems not to rely on an altered cell fate decision between IFS and polar follicle

cells, which have been shown to derive from common precursors (Ruohola et al., 1991) (data not shown). Even though the IFS cells do exist in the rudimentary ovarioles of *bab* mutant ovaries, they are not able to arrange into a stack. This phenotypic trait is similar to the failure to form TFs in the larval ovary.

DISCUSSION

Ovariole development begins with formation of the TFs in the ovary during the third larval instar. We analyzed the development of the two-dimensional array of TFs and compare this process with the formation of the BSs and IFSs. Furthermore, we show that *bab* is crucial for TF formation and the subsequent morphogenesis of the ovary.

Cell stacks in the ovary form by cell recruitment

TFs together with BSs and IFSs represent a specialized tissue type containing disc-shaped cells organized in an one-dimensional stack. Single rows of cells could form by different mechanisms. They could form by polar cell division of a stem cell, which produces a string of daughter cells as is seen with germinal bandlets derived from teloblasts in a leech embryo (Weisblat and Shankland, 1985), or they could form by consecutive divisions of aligned cells. In both cases, cells are directly clonally related and cell clones are found in specific and repeated spatial patterns. Alternatively, single rows of cells could form by recruitment of primordial cells. An example is the formation of the notochord in ascidian embryos (Nishida and Satoh, 1985). We have shown that TFs are composed of cells of different lineages that are randomly mixed. This rules out the possibility that a TF derives from a single progenitor cell and argues strongly for a recruitment mechanism. Clonally mixed cell stacks also indicate that cell rearrangement plays a role in the formation of TFs. We believe that the BSs and IFSs also form by cell recruitment because both stalks develop through the reorganization of a preexisting cell population.

Cell stacks form through cell rearrangement

Cell rearrangement is a powerful morphogenetic mechanism through which local cell behavior can result in the change of the shape of a whole tissue. It is responsible for convergence and extension, which drives gastrulation of sea urchin (Hardin, 1989), zebrafish (Warga and Kimmel, 1990) and *Xenopus* (Wilson and Keller, 1991) and leads to the transformation of the spherical shape of the egg into the axial structure of a chordate embryo (for review see Keller et al., 1992) and to the analogous extension of the germband in the *Drosophila* embryo (Irvine and Wieschaus, 1994). The basis of the convergence of a cell population is a change towards a flattened cell shape and towards a bidirectional motility of the involved cells, which enables the cells to intercalate between each other. The intercalation leads to an extension of the tissue perpendicular to the cell movement. A hallmark for this type of morphogenetic movement is the apparently paradoxical situation that cells flatten in the same direction in which the whole tissue will eventually extend. This is different from the process where the change in tissue shape reflects the change in cell shape as shown for the evagination of the imaginal discs in *Drosophila* (Condic et al., 1991). By analyzing the different developmental stages in BS and IFS formation, we could show that these single rows of cells derive from a primordium which is initially much shorter and several cell diameters wide. During the transition to a single row, cells achieve a flattened shape and intercalate perpendicular to the direction the tissue will extend.

If cells are freely motile in two directions their movements would equilibrate each other and the tissue would not change in shape. However, convergence can be achieved by a restriction in the motility of the cells along the tissue boundary, so that these cells can not leave the boundary, as it has been theoretically proposed (Weliky et al., 1991) and experimentally demonstrated in tissue explants of *Xenopus* gastrulae (Wilson and Keller, 1991). The primordium of each BS or IFS is enclosed by a thick basement membrane prior to stalk formation (King, 1970). During stalk formation, the BS and IFS cells that flank the tissue boundary have a wedge-shaped appearance suggesting that these cells have established stable contact to the basement membrane with one side and use their free protrusive side for intercalation. When a single row of cells is formed, each cell is in contact with the basement membrane along its circumference and as a consequence takes on a disc-shaped appearance with a blunt margin all around. The formation of the BS and IFS in the ovary of *Drosophila*

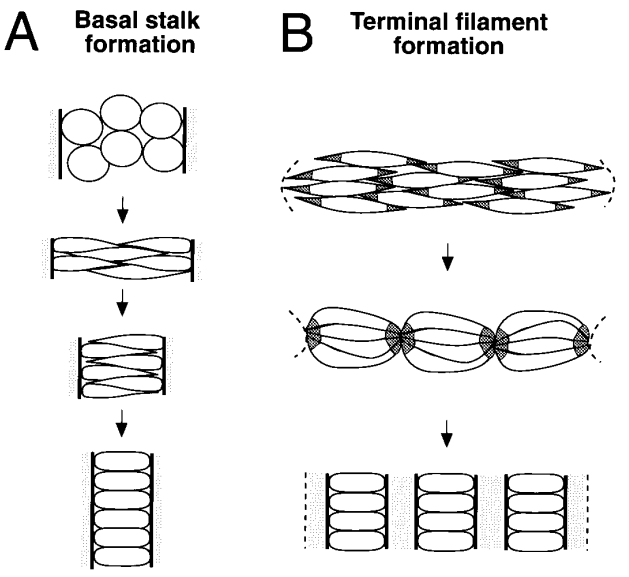

Fig. 12. Model that compares TF formation and BS formation. (A) A BS (or IFS) forms by a classic convergence and extension mechanism. A group of BS cells that will give rise to a single stack is set apart and surrounded by a basement membrane (black bar) and an epithelial sheath (shaded). The original round cells flatten, intercalate, contact the basement membrane and form a stack of disc-shaped cells. (B) TF formation involves cell sorting in addition to convergence and extension. Three TFs are shown emerging from a uniform cell population. Convergent intercalation of cells causes the formation of a furrow at the ovary surface (dashed line). The tapered margins of the TF cells (strongly shaded) are more adhesive to each other than to the remaining cell surface, which leads to a sorting of the cells and eventually to distinct eye-shaped cell clusters. When a basement membrane (black bar) and the apical cells (slightly shaded) separate the clusters, the spindle-shaped cells are transformed into disc-shaped cells by changing from cell-cell adhesion towards cell-substrate adhesion (see text for further discussion).

appears to be an example of classic convergence and extension (Fig. 12A).

Terminal filament formation involves cell sorting

TFs develop from an apparently uniform cell population that has not been divided into subpopulations prior to stalk formation. Therefore, in contrast to BS and IFS development, the formation of a single TF can not be regarded as a process independent from the formation of the neighboring TFs. The two-dimensional array of TFs arises through a morphogenetic process in which TFs develop progressively along the medial-lateral axis of the ovary but appear simultaneously along the dorsal-ventral axis. Along the dorsal-ventral axis, an initial movement of TF cells leads to aggregates where cells of future neighboring stacks are interdigitated. Subsequently the TF cells sort out by reverse intercalation and form separated clusters. Based on tissue cultures, it has been proposed that sorting-out of different cell types is due to differences in their adhesive properties (Townes and Holtfreter, 1955; Steinberg, 1970), and it has been shown that cells sort out from one another differing in the expression of different cadherin adhesion molecules (Nose et al., 1988; Friedlander et al., 1989) or in the expression of different levels of a single cadherin type (Friedlander et al., 1989; Steinberg and Takeichi, 1994). A sorting of identical cells, as seen with TF cells, might rely on a differential distribution of cell adhesion molecules on the surface of individual cells. The most striking feature in TF formation is the appearance of an eye-shaped cell cluster immediately after the cell sorting process. Eye cluster formation results from a strong bundling of the TF cell margins, which might prevent further intercalation movements so that the TF cells become trapped in a particular cluster. The strong bundling of the TF is accompanied by a high concentration of actin filaments and the β-catenin and plakoglobin-related protein Arm in the tapered ends of the cells. In mammalian cell cultures accumulation of β-catenin and plakoglobin at the cell surface correlates with an increased degree of cadherin-mediated adhesion between cells (Bradley et al., 1993; Hinck et al., 1994), and the *arm* mutant phenotype in oogenesis is consistent with the proposed role of Arm in cell adhesion (Peifer et al., 1993). Taken together, it suggests that the margins of TF cells exert a highly attractive force upon each other. If the adhesion between the margins of the TF cells is higher than the adhesion along the remaining cell surface, it is possible that a TF cell intercalates until its tapered margin has gained contact to the margins of other TF cells, which leads to a sorting of the cells until they are organized into distinct cell clusters. That a moderate level of adhesion promotes cell motility but a high level of adhesivity prevents cell movements has been shown for cell-substrate interactions (e.g. DiMilla et al., 1993). In summary, we propose that differences in the adhesive properties along the surface of an individual cell play a critical role in the pattern forming process that facilitates the development of multiple TFs from a common cell pool (Fig. 12B).

There is no indication that non TF cells are involved in the development of distinct TF cell clusters. Distinct clusters have already formed before the apical cells penetrate the TF cell region suggesting that the formation of the two-dimensional array of TF cell stacks is based on the morphogenetic properties of TF cells. However, the transformation of the eye-shaped cluster towards a mature TF might be related to the invasion of the apical cells and the formation of a basement membrane which provides a new substrate for the TF cell margins. The change towards a disc-like cell shape with a circular blunt margin and the relocalization of Arm, but not of F-actin, away from these margins suggests a transition from cell-cell towards cell-substrate adhesion.

bab is required for ovary morphogenesis

bab plays a central role in ovary morphogenesis and is the first gene described to control this process. *bab* mutant females are sterile and have small and disorganized ovaries. The absence of ovarioles in *bab* mutant ovaries results from developmental defects in morphogenesis during the third larval instar and early pupal stages. The primary defect appears to be the failure to form TFs, which correlates with the specific expression of the Bab protein in the nuclei of TF cells, beginning with their appearance during the third larval instar.

Our phenotypic analysis shows that *bab* is required for TF formation. *bab* mutant TF cells have an abnormal shape, are not able to form normal stacks, and appear to be partially located in ectopic positions in the ovary, indicating that they are affected in their morphogenetic properties. This phenotype is cell autonomously expressed. In addition to the TFs, other somatic cell populations in the ovary are also affected at the onset of metamorphosis. The BS primordium and the apical cell population are strongly reduced in size. Because the Bab protein is only detected in TF cells and appears to be cell autonomously required, one possibility is that the absence of TFs is responsible for these additional phenotypic traits. Alternatively, *bab* may be directly involved in the proper development of other somatic cell types in the ovary, including the IFS cells. The bab^{P} enhancer trap expresses β-gal not only in TFs but also at lower levels in BSs, in forming IFSs, as well as in some other somatic cells of the adult ovary (Sahut, Godt, Laski and Couderc, unpublished data). In addition, the recently identified BTB-II transcript that is related to *bab*, based on the same chromosomal map position, sequence homology and an overlapping expression pattern (Zollman et al., 1994), is expressed in TFs, the apical cells and the BS primordium of a prepupal ovary (unpublished observations), and *bab* mutations may affect both transcripts.

A characteristic defect of oogenesis in *bab* mutants is fused follicles. This is at least partially attributable to a failure in IFS formation, although the IFS cells, identified with a genetic cell marker, are present at their proper location. IFS cells, like TF cells, are not able to arrange into stacks. This is different from the phenotype of mutations in the neurogenic genes, where the fusion of follicles results from the absence of IFS cells due to an altered cell fate (Ruohola et al., 1991). Therefore, if bab acts directly in IFS development it is expected to function downstream of the neurogenic genes in this process.

We thank Jean-Louis Couderc, Ulrich Tepass and the UCLA Embryology Club for refreshing discussions and Ulrich Tepass, John Fessler and Patricia Green for very helpful comments on the manuscript. We are grateful to Wen Juan Yu for excellent technical assistance. We thank Cahir O'Kane for the bab^{A128} line, Hannele Ruohola-Baker and Yuh Nuang Jan for providing the B1-93F, FLP and FRT2A fly stocks, Corey S. Goodman for generous supply of Fasciclin III antibody, and Mark Peifer for the gift of Armadillo antibody. F. A.

L. is a Pew Scholar in the Biomedical Sciences. Funding was also provided by the NIH.

REFERENCES

Ashburner, M. (1989). Drosophila. *A Laboratory handbook.* Cold Spring Harbor Laboratory Press.

Bard, J. B. L. (1990). *Morphogenesis: the Cellular and Molecular Processes of Developmental Anatomy.* New York: Cambridge University Press.

Bellen, H. J., O' Kane, C. J., Wilson, C., Grossniklaus, U., Pearson, R. K., and Gehring, W. J. (1989). P-element-mediated enhancer detection: a versatile method to study development in *Drosophila*. *Genes Dev.* **3**, 1288-1300.

Bradley, R. S., Cowin, P. and Brown, A. M. C. (1993). Expression of Wnt-1 in PC12 cells results in modulation of plakoglobin and E-cadherin and increased cellular adhesion. *J. Cell Biol.* **123**, 1857-1865.

Brower, D. L., Smith, R. J. and Wilcox, M. (1980). A monoclonal antibody specific for diploid epithelial cells in *Drosophila*. *Nature* **285**, 403-405.

Brower, D. L., Smith, R. J. and Wilcox, M. (1981). Differentiation within the gonads of *Drosophila* revealed by immunofluorescence. *J. Embryol. Exp. Morph.* **63**, 233-242.

Campos-Ortega, J. A. and Hartenstein, V. (1985) *The Embryonic Development of* Drosophila melanogaster. Berlin: Springer.

Condic, M. L., Fristrom, D. and Fristrom, J. W. (1991). Apical cell shape changes during *Drosophila* imaginal leg disc elongation: a novel morphogenetic mechanism. *Development* **111**, 23-33.

Costa, M., Wilson, E. T. and Wieschaus, E. (1994). A putative cell signal encoded by the folded gastrulation gene coordinates cell shape changes during *Drosophila* gastrulation. *Cell* **76**, 1075-1089.

DiMilla, P. A., Stone, J. A., Quinn, J. A., Albelda, S. M. and Lauffenburger, D. A. (1993). Maximal migration of human smooth muscle cells on fibronectin and type IV collagen occurs at an intermediate attachment strength. *J. Cell Biol.* **122**, 729-737.

Friedlander, D. R., Mège, R. M., Cunnigham, B. A. and Edelman, G. M. (1989). Cell sorting-out is modulated by both the specificity and the amount of different cell adhesion molecules (CAMs) expressed on cell surfaces. *Proc. Natl. Acad. Sci. USA* **86**, 7043-7047.

Godt, D., Couderc, J. L., Cramton, S. E. and Laski, F. A. (1993). Pattern formation in the limbs of *Drosophila: bric à brac* is expressed in both a gradient and a wave-like pattern and is required for specification and proper segmentation of the tarsus. *Development* **119**, 799-812.

Golic, K. G. (1991). Site-specific recombination between homologous chromosomes in *Drosophila*. *Science* **252**, 958-961.

Hardin, J. (1989). Local shifts in position and polarized motility drive cell rearrangement during sea urchin gastrulation. *Dev. Biol.* **136**, 430-445.

Hinck, L., Nelson, W. J. and Papkoff, J. (1994). Wnt-1 modulates cell-cell adhesion in mammalian cells by stabilizing β-catenin binding to the cell adhesion protein cadherin. *J. Cell Biol.* **124**, 729-741.

Irvine, K. D. and Wieschaus, E. (1994). Cell intercalation during *Drosophila* germband extension and its regulation by pair-rule segmentation genes. *Development* **120**, 827-841.

Keller, R., Shih, J. and Domingo, C. (1992). The patterning and functioning of protrusive activity during convergence and extension of the *Xenopus* organiser. *Development* Supplement, 81-91.

Kerkis, J. (1930). The growth of the gonads in *Drosophila melanogaster*. *Genetics* **16**, 212-224.

Kerkis, J. (1933). Development of gonads in hybrids between *Drosophila melanogaster* and *Drosophila simulans*. *J. Exp. Zool.* **66**, 477-509.

King, R. C., Aggarwal, S. K. and Aggarwal, U. (1968). The development of the female *Drosophila* reproductive system. *J. Morph.* **124**, 143-166.

King, R. C. (1970). *Ovarian Development in* Drosophila melanogaster. New York: Academic press.

Kuo, C. H., Gilon, H., Blumenthal, A. B. and Sedat, J. W. (1982) A library of monoclonal antibodies to nuclear proteins from *Drosophila melanogaster* embryos. *Exp. Cell Res.* **142**, 141-154.

Leptin, M. and Grunewald, B. (1990). Cell shape changes during gastrulation in *Drosophila*. *Development* 1**10**, 73-84.

Lindsley, D. L., and Zimm, G. G. (1992). *The Genome of Drosophila melanogaster*. New York: Academic press, INC., Harcourt Brace Jovanovich, Publishers.

Mahowald, A. P. and Kambysellis, M. P. (1980). Oogenesis. In *The Genetics and Biology of* Drosophila vol. 2d (eds M. Ashburner and T. R. F. Wright), pp. 141-224. New York: Academic Press.

Nishida, H. and Satoh, N. (1985). Cell lineage analysis in ascidian embryos by intracellular injection of a tracer enzyme. *Dev. Biol.* **110**, 440-454.

Nose, A., Nagafuchi, A. and Takeichi, M. (1988). Expressed recombinant cadherins mediate cell sorting in model systems. *Cell* **54**, 993-1001.

Patel, N. H., Snow, P. M. and Goodman, C. S. (1987). Characterization and cloning of Fasciclin III: A glycoprotein expressed on a subset of neurons and axon pathways in *Drosophila*. *Cell* **48**, 975-988.

Peifer, M. and Wieschaus, E. (1990). The segment polarity gene *armadillo* encodes a functionally modular protein that is the *Drosophila* homolog of human plakoglobin. *Cell* **63**, 1167-1178.

Peifer, M. (1993). The product of the *Drosophila* segment polarity gene *armadillo* is part of a multi-protein complex resembling the vertebrate adherens junction. *J. Cell Science* **105**, 1-8.

Peifer, M., Orsulic, S., Sweeton, D. and Wieschaus, E. (1993). A role for the *Drosophila* segment polarity gene *armadillo* in cell adhesion and cytoskeletal integrity during oogenesis. *Development* **118**, 1191-1207.

Peifer, M., Sweeton, D., Casey, M. and Wieschaus, E. (1994). Wingless signal and Zeste-white 3 kinase trigger opposing changes in the intracellular distribution of Armadillo. *Development* **120**, 369-380.

Reuter, R., Grunewald, B. and Leptin, M. (1993). A role for the mesoderm in endodermal migration and morphogenesis in *Drosophila*. *Development* **119**, 1135-1145.

Ruohola, H., Bremer, K. A., Baker, D., Swedlow, J. R., Jan, L. Y. and Jan, Y. N. (1991). Role of neurogenic genes in establishment of follicle cell fate and oocyte polarity during oogenesis in *Drosophila*. *Cell* **66**, 433-449.

Snodgrass, R. E. (1935). *Principles of Insect Morphology*. New York: McGraw-Hill book company, INC.

Spradling, A. (1993). Developmental genetics of oogenesis. In Drosophila *Development*. vol 1 (eds. M. Bate and A. Martinez-Arias), pp. 1-70. Cold Spring Harbor NY: Cold Spring Harbor Press.

Steinberg, M. S. (1970). Does differential adhesion govern self-assembly processes in histogenesis? Equilibrium configurations and the emergence of a hierarchy among populations of embryonic cells. *J. Exp. Zool.* **173**, 395-434.

Steinberg, M. S. and Takeichi, M. (1994). Experimental specification of cell sorting, tissue spreading, and specific spatial patterning by quantitative differences in cadherin expression. *Proc. Natl. Acad. Sci. USA* **91**, 206-209.

Tepass, U. and Hartenstein, V. (1994). Epithelium formation in the *Drosophila* midgut depends on the interaction of endoderm and mesoderm. *Development* **120**, 579-590.

Townes, P. S., and Holtfreter, J. (1955). Directed movements and selective adhesion of embryonic amphibian cells. *J. Exp. Zool.* **128**, 53-120.

Warga, R. M. and Kimmel, C. B. (1990). Cell movements during epiboly and gastrulation in zebrafish. *Development* **108**, 569-580.

Weisblat, D. A. and Shankland, M. (1985). Cell lineage and segmentation in the leech. *Phil. Trans. Roy. Soc. Lond.* **B312**, 39-56.

Weliky, M., Minsuk, S., Keller, R. and Oster, G. (1991). Notochord morphogenesis in *Xenopus laevis*: simulation of cell behavior underlying tissue convergence and extension. *Development* **113**, 1231-1244.

Wilson, P. and Keller, R. (1991). Cell rearrangement during gastrulation of *Xenopus*: direct observation of cultured explants. *Development* **112**, 289-300.

Zollman, S., Godt, D., Prive, G. G., Couderc, J. L. and Laski, F. A. (1994). The BTB domain, found primarily in zinc finger proteins, defines an evolutionarily conserved family that includes several developmentally regulated genes in *Drosophila*. *Proc. Natl. Acad. Sci. USA*, **91**, 10717-10721.

(Accepted 13 October 1994)